High performance microspherical activated carbons for methane storage and landfill gas or biogas upgrade

Article *in* Journal of Materials Chemistry A · October 2014

DOI: 10.1039/C4TA0342J

CITATIONS
31

READS
1,105

5 authors, including:

Ana Mestre
University of Lisbon
76 PUBLICATIONS **2,485** CITATIONS
SEE PROFILE

Cristina Freire
University of Porto Faculty of Sciences
362 PUBLICATIONS **10,448** CITATIONS
SEE PROFILE

João Pires
University of Lisbon
212 PUBLICATIONS **6,320** CITATIONS
SEE PROFILE

Ana P Carvalho
University of Lisbon
196 PUBLICATIONS **5,715** CITATIONS
SEE PROFILE

Journal of Materials Chemistry A

PAPER

Cite this: J. Mater. Chem. A, 2014, 2, 15337

High performance microspherical activated carbons for methane storage and landfill gas or biogas upgrade†

Ana S. Mestre,*[ab] Cristina Freire,[b] João Pires,[a] Ana P. Carvalho[a] and Moisés L. Pinto*[c]

Received 25th June 2014
Accepted 16th July 2014

DOI: 10.1039/c4ta03242j

www.rsc.org/MaterialsA

Microspherical activated carbons were successfully prepared *via* a novel synthetic route that involves hydrothermal carbonization of a renewable material, sucrose, and activation with K_2CO_3. The use of K_2CO_3 resulted in better yields (~50%) and the retention of the spherical shape of the hydrochar, while with the less environmentally desirable and commonly used activating agent, KOH, the process occurs at the expense of the spherical morphology. The superior performance of the K_2CO_3 activated samples for methane storage and upgrade of landfill gas or biogas results from the combination of several key properties including high packing densities (~0.9 g cm^{-3}), high surface areas (up to 1400 m^2 g^{-1}) and micropore sizes suitable for methane storage and selective CO_2–CH_4 separation. In fact, the micropore size distributions assessed from CO_2 adsorption data through a methodology not imposing a Gaussian distribution gave meaningful values to explain both the selectivity and storage capacity of samples. Sample activated with K_2CO_3 at 800 °C presenting micropore sizes ~0.8 nm and high packing density has high volumetric methane uptake (90 (V/V) at 1000 kPa), close to the best activated carbons reported in the literature. Sample activated with K_2CO_3 at 700 °C has narrower micropores (~0.5 nm) and presents a remarkable selectivity (4–7) in CO_2–CH_4 mixtures for the upgrade of methane based fuels, like natural gas, landfill gas, and biogas. Although a superactivated carbon (~2400 m^2 g^{-1}) was obtained with KOH activation, the low packing density and wider micropores rendered it less effective for both methane storage and upgrade.

Introduction

The search for renewable energy sources is becoming increasingly important due to global warming and climate change effects that are currently becoming more severe. In this context, fuels based on renewable sources, like landfill gas and biogas, which are rich in methane, need to be further explored regarding both production and use. Two main technological steps are involved in the spreading of these methane based fuels. The first is the purification or upgrading of the methane content on these gases and the second is methane storage at high densities and low to moderate pressures for easy application in the automotive industry. In the present work, we explore the merits of microspherical activated carbons prepared from sucrose-based hydrochars in applications to overcome these two challenges.

Methane separation from carbon dioxide is the main step in the upgrading of natural gas, landfill gas and biogas to achieve fuel grade quality, and to avoid corrosion during transport and storage.[1] It is often mandatory to purify these gases before their use in high value applications because they may contain large amounts of carbon dioxide (40–65%).[2–4] Other contaminants are also present, although in lower concentrations, and are easier to separate from methane. For example, the minimum fuel quality for compressed natural gas driven vehicles now corresponds to the G25 reference test fuel (85% methane, 14% nitrogen).[5] Thus, enrichment of methane is a pre-requisite, which is essentially achieved by carbon dioxide removal. Regarding landfill gas and biogas, prevention of their uncontrolled emission to the atmosphere is environmentally important because the global warming potential (GWP) of CH_4 is 21 times higher than that of CO_2.[6,7] Separation studies of CH_4 from CO_2 by adsorption processes using several types of adsorbent materials, like alumina, activated carbons, zeolites and porous clays, were revised in the introduction of recent papers.[8–10]

Storage of methane by compression requires multi-stage compression up to 20 MPa to achieve a practical storage capacity in a given tank, implying expensive compression units

[a]Centro de Química e Bioquímica, Faculdade de Ciências, Universidade de Lisboa, 1749-016 Lisboa, Portugal. E-mail: asmestre@fc.ul.pt; Fax: +351 217500088

[b]REQUIMTE, Departamento de Química e Bioquímica, Faculdade de Ciências, Universidade do Porto, 4169-007, Portugal

[c]Department of Chemistry, CICECO, University of Aveiro, 3810-193 Aveiro, Portugal. E-mail: moises.pinto@ua.pt; Fax: +351 234401470

† Electronic supplementary information (ESI) available: Details on analysis of α_S plots and adsorption modelling; additional methane and carbon dioxide adsorption isotherms in the low pressure region at 25 °C. See DOI: 10.1039/c4ta03242j

and storage tanks, and considerable energy consumption. Another method of storage is gas adsorption at relatively low pressure in a lightweight cylinder filled with an adsorbent material. This method is attractive because the adsorbent can be filled with the gas using an inexpensive single-stage compressor, thus demanding less energy consumption. Methane storage in activated carbons at low to moderate pressures has been considered as a very promising alterative to compression and their fundamental aspects are reasonably studied.[11,12] Carbon materials have been successfully used in methane storage and landfill gas or biogas upgrading mainly due to their large specific surface areas, microporosity tailoring, and high packing densities. These properties are allied to the possibility of being produced from largely available renewable biomass, which make them less expensive than other microporous adsorbent materials (*i.e.* zeolites or metal–organic frameworks).

Superactivated carbons, prepared by chemical activation with KOH of hydrochars obtained from hydrothermal carbonization (HTC) of carbohydrates, polysaccharides or biomass, have shown very high adsorption capacities for CO_2 capture[13,14] or CH_4 storage.[13] However, these materials have lower packing densities than, for instance, anthracite-derived carbons with similar micropore networks,[15] which is a disadvantage for their use in storage or separation processes, since an adsorbent with low packing density requires bigger storage containers or separation towers.

Due to our experience in using K_2CO_3 as an activating agent,[16–23] recently we have been interested in extending our studies to the activation of spherical hydrochars with this compound aiming at the preparation of spherical activated carbons.[24] K_2CO_3 is an alternative to KOH with the advantage that carbonate mediated activation is less extensive and K_2CO_3 is an environmental friendly activating agent[25] compared to $ZnCl_2$, H_3PO_4, and KOH, the most commonly reported chemical activating agents.[26] So, to combine the development of the microporosity and the preservation of the hydrochar spherical morphology, K_2CO_3 is a promising activating agent.

The objective of the present work was to test three sucrose-derived activated carbons for methane storage or upgrade from landfill gas or biogas. The samples were selected from a larger set of activated carbons prepared from hydrochars in order to have materials presenting highly developed and tailored microporosity, preferentially allied with spherical morphology to attain high packing densities. The use of K_2CO_3 as an activating agent of spherical hydrochars proved to be crucial in obtaining high performance adsorbents for methane storage and also for natural, landfill gas or biogas upgrade.

Experimental

Activated carbon preparation

The hydrochar was prepared introducing 15 cm^3 of 1.5 mol dm^{-3} sucrose (Analar Normapur, >99%) aqueous solution in a Teflon-lined stainless steel autoclave. The autoclave was placed in an oven (Medline Scientific Limited, model ON-02G), which had been pre-heated at 190 °C and hydrothermal carbonization (HTC) was performed for 5 h. The autoclave was cooled down to room temperature and the powder (hydrochar S) was washed with distilled water and acetone, and dried at 60 °C. Activated carbon samples SC800 and SH800 were prepared with, respectively, K_2CO_3 and KOH. The activation was performed by impregnating in solution (~10 cm^3) 1 g of hydrochar with 4 g of K_2CO_3 (Aldrich, 99%) for SC800, or KOH (Panreac, 85%) for SH800, for 2 h at room temperature, and then the samples were dried at 100 °C in a ventilated oven. Activation occurred in a horizontal furnace (Thermolyne, model 21100) at 800 °C for 1 h under a N_2 flow of 5 cm^3 s^{-1} after a heating ramp of 10 °C min^{-1}. Sample SC700P was prepared by physical impregnation of 1 g of hydrochar with 4 g of ground K_2CO_3 and activated at 700 °C under the experimental conditions described above. After cooling under N_2 flow, the samples were thoroughly washed with distilled water until pH 7, and finally dried overnight at 100 °C being cooled in a desiccator.

Activated carbon characterization

Solid morphology characterization was performed with a scanning electron microscope (SEM) (JEOL, mod. 7001F) using an accelerating voltage of 25 kV.

The porous texture characterization of the carbon adsorbents was made by N_2 and CO_2 adsorption at −196 and 0 °C, respectively. The N_2 adsorption isotherms were obtained in an automatic apparatus Micromeritics ASAP 2010 while the CO_2 adsorption experiments were carried out using a conventional volumetric apparatus equipped with an MKS-Baratron (310BHS-1000) pressure transducer (0–133 kPa). In any case, before the isotherm measurement, the samples (~50 mg) were outgassed overnight at 120 °C under vacuum better than 10^{-2} Pa. From N_2 adsorption data the apparent surface area (A_{BET}) was determined through the Brunauer–Emmett–Teller (BET) equation ($0.05 < p/p^0 < 0.15$)[27] and the total pore volume (V_{total}) was assessed by the Gurvich rule,[28] corresponding to the volume of N_2 adsorbed at $p/p^0 = 0.975$. The microporosity was analysed applying the Dubinin–Radushkevich (DR) equation[27] to the N_2 and CO_2 adsorption data ($W_{0\ N_2}$ and $W_{0\ CO_2}$, respectively). The α_S method was also applied to the N_2 adsorption data, taking as a reference the isotherm reported by Rodríguez-Reinoso *et al.*,[29] and the volumes of total micropores ($V_{\alpha\ total}$), ultramicropores ($V_{\alpha\ ultra}$) and supermicropores ($V_{\alpha\ super}$) were assessed according to the description presented in the ESI.† The mesoporous volume (V_{meso}) corresponds to the difference between V_{total} and $V_{\alpha\ total}$.

Densities of the activated carbons were determined by two distinct methodologies described in the literature.[12,15] The tap density was measured by filling a graduated cylinder with the adsorbent and vibrating, while the packing density was determined by pressing the adsorbent in a mould at a pressure of 550 kg cm^{-2}. In all the cases, around 0.5 g was used to perform the assays. The measurements were repeated at least three times and the densities presented correspond to the mean value. The N_2 adsorption isotherms of the samples obtained after packing revealed that the apparent surface area decreases less than 10% after this procedure.

CH_4 and CO_2 adsorption measurements above atmospheric pressure

The adsorption isotherms of CO_2 and CH_4 (Air Liquide, 99.995%) were determined using a laboratory made stainless steel volumetric apparatus, with a pressure transducer (Pfeiffer Vacuum, APR 266), equipped with a rotary/diffusion pump system which allowed a vacuum greater than 10^{-2} Pa. The temperature of the apparatus and adsorption cell was maintained with a water bath (Grant, GD 120) at 25.00 ± 0.05 °C. Before adsorption experiments, the samples were degassed as previously described for N_2 and CO_2 adsorption assays. The non-ideality of the gas phase was taken into account using the second and third virial coefficients to calculate the adsorbed amounts. The selectivity and phase diagrams of binary CO_2–CH_4 mixtures were estimated by a method based on the Ideal Adsorbed Solution Theory (IAST), which was described in detail in previous studies[9,10] and is summarized in the ESI.†

Results and discussion

Activated carbon properties

The activation of the sucrose-derived hydrochars with K_2CO_3 and KOH at 800 °C originates adsorbents with well-developed porosity presenting type I isotherm characteristic of microporous solids (Fig. 1(a)). The sample physically impregnated with K_2CO_3 and activated at 700 °C (SC700P) is, as expected, the carbon with the less developed microporous structure, while KOH activation led to the material with the most developed micropore network. Activation with KOH produces a material with the highest specific surface area and pore volumes (Table 1). However, when compared with the K_2CO_3-activated carbons, the SH800 sample presents the lowest preparation yield (13% *versus* 45–51%) and is the only sample that did not maintain the spherical shape of the hydrochar (Fig. 2).

According to the literature, the KOH activation mechanism involves a series of reactions that start at temperatures relatively low (~400 °C) leading to the formation of H_2O, CO_2, CO and H_2.[30–32] Some of these compounds are commonly used as physical activating agents and so the consumption of the carbon matrix starts at ~400 °C. Another reaction product of KOH activation is K_2CO_3 which will decompose only at temperatures between 700 and 800 °C, resulting in the formation of metallic K, which remains intercalated in the carbon structure. The activation occurs due to redox reactions where C from the carbon matrix is oxidized and the activating agent is reduced (from K^+ to metallic K). The removal of metallic K during the washing step unblocks the micropore network.

When K_2CO_3 is used as the activating agent the reaction starts only at around 800 °C[30] and the reactions at lower temperatures observed in the case of KOH are absent. The use of carbonate will then allow a less extensive consumption of the carbon matrix resulting in a lower porosity development, but gathering the conditions to maximize the material density. Thus, the higher activation yield, less extensive development of the microporous network (Table 1) and the preservation of hydrochar spherical morphology (Fig. 2) observed for the

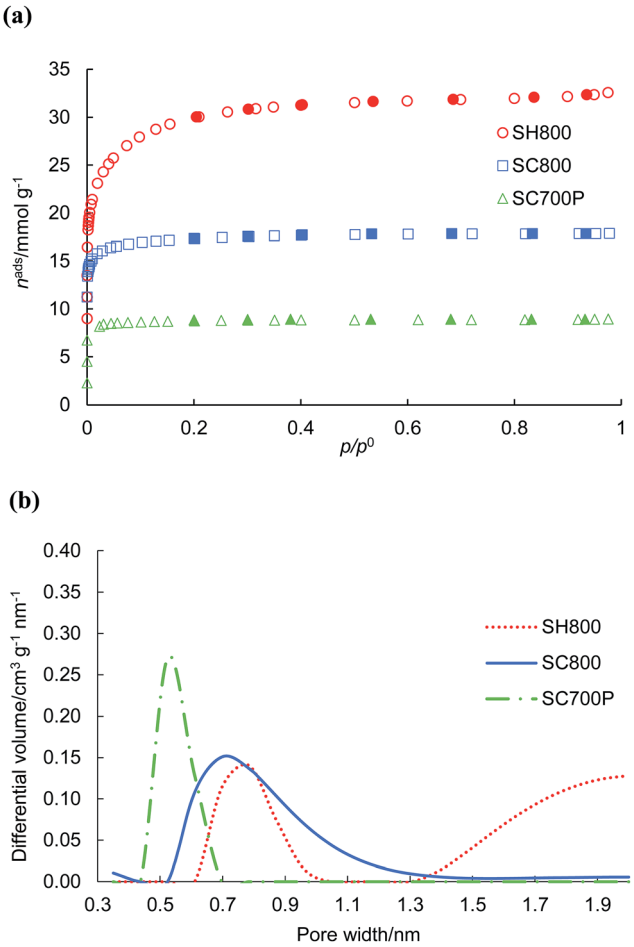

Fig. 1 (a) N_2 adsorption–desorption isotherms at −196 °C, closed symbols are the desorption points; (b) micropore size distributions of the activated carbon, obtained by fitting CO_2 adsorption data at 0 °C to the method described by Pinto *et al.*[34]

K_2CO_3-activated carbons (SC800 and SC700P) are in line with differences between the activation mechanism of K_2CO_3 and KOH and reveal the advantages of K_2CO_3 activation of spherical hydrochars.

Regarding the microporous structure, the α_S method results (Table 1) show that while the sample activated with KOH (SH800) has exclusively larger micropores (supermicropores – widths between 0.7 and 2 nm), the K_2CO_3-activated carbons present both narrow and wider micropores, with higher percentage of narrow micropores (ultramicropores – widths <0.7 nm). These results are expected according to the distinct activation mechanisms.

The volumes of micropores assessed by applying the DR equation to the N_2 and CO_2 data are also in line with the previous analysis: sample SH800 has $W_{0\ N_2} > W_{0\ CO_2}$, which is indicative of high activation degrees and the presence of wider micropores, while samples activated with K_2CO_3 (SC800 and SC700P) have $W_{0\ N_2} < W_{0\ CO_2}$, which is indicative of the presence of narrower micropores.[33] Further characterization of the activated carbons by micropore size distributions (Fig. 1(b)), assessed by fitting CO_2 adsorption data at 0 °C to the method

Table 1 Nanotextural properties of the activated carbons and preparation yield (η)

				α_S method			DR equation		
Sample	A_{BET} ($m^2\ g^{-1}$)	V_{total}[a] ($cm^3\ g^{-1}$)	V_{meso}[b] ($cm^3\ g^{-1}$)	$V_{\alpha\ total}$ ($cm^3\ g^{-1}$)	$V_{\alpha\ ultra}$ ($cm^3\ g^{-1}$)	$V_{\alpha\ super}$ ($cm^3\ g^{-1}$)	$W_{DR\ N_2}$ ($cm^3\ g^{-1}$)	$W_{DR\ CO_2}$ ($cm^3\ g^{-1}$)	η[c] (%)
SH800	2431	1.14	0.06	1.08	0.00	1.08	0.90	0.71	13
SC800	1375	0.63	0.01	0.62	0.35	0.27	0.58	0.65	45
SC700P	694	0.31	0.00	0.31	0.23	0.08	0.31	0.41	51

[a] Evaluated at $p/p^0 = 0.975$ in the N_2 adsorption isotherms at −196 °C. [b] Difference between V_{total} and $V_{\alpha\ total}$. [c] Yield is defined as: g of activated carbon per 100 g of hydrochar.

described by Pinto *et al.*,[34] corroborates the assumptions made above. Carbon SH800 has a bimodal micropore size distribution with pores mainly in the supermicropore region, whereas samples SC800 and SC700P present monomodal distributions centered at ~0.7 and ~0.5 nm, respectively. It is noteworthy that carbon SC800 has a broad distribution of pores around 0.8 nm that are considered to maximize methane uptake and its delivery at ambient pressure.[12] Although presenting the less developed porous network, sample SC700P has a very narrow micropore size distribution which, as it will be discussed later on, plays a very important role in the separation of the CO_2–CH_4 mixture.

Envisaging the use of these samples for carbon storage, it is also essential to evaluate their densities, because the materials used for gas storage must also have high storage capacity on a volumetric basis. Both tap and packing density values are presented in Table 2, and reveal that K_2CO_3-activated carbons have much higher densities. In the case of packing densities, the values determined for the K_2CO_3-activated samples are two to three times higher than that obtained for the sample activated with KOH.

In summary, although presenting lower micropore volumes than samples activated with KOH, the carbons prepared by K_2CO_3 activation of the hydrochar have preparation yields about four times higher and very high packing densities, most certainly related to the preservation of the spherical morphology after the activation, allied to monomodal micropore size distributions centered below 0.8 nm; all these features being fundamental requisites for materials to be used in gas storage.

Methane and carbon dioxide adsorption

The adsorption isotherm profiles of CH_4 and CO_2, up to 1000 kPa (Fig. 3), show that sample SC700P seems to be reaching a plateau at high pressures, indicating saturation of the porosity, for the adsorption of both gases. For the other two samples, especially in the case of SH800, the materials are not saturated at the highest pressures attained. This indicates that the highest pressure used was sufficient to saturate the material with the narrower pores (SC700P), but not the other two materials which have wider pores (SH800 and SC800).

The highest uptake for CO_2 was attained by sample SH800, which is in line with the significantly higher apparent surface area and pore volume of this sample compared to the others (Table 1). For the K_2CO_3-activated carbons the maximum adsorbed amounts also follow the surface area and pore volume trends. In contrast, in the low pressure region carbon SH800 presents lower CO_2 uptakes (~25%) than the K_2CO_3-activated carbons (Fig. S2†). This behaviour is probably a consequence of the wider micropores of this sample (Fig. 1 and Table 1), which are not so effectively interacting with the CO_2 molecules in the low pressure region. This issue is further discussed below.

The results of CH_4 adsorption present a different trend from those of CO_2, in the studied pressure range. Carbon SC800 adsorbed higher amounts than the other samples, although it seems likely from the isotherm configuration that the isotherm of SH800 will cross the isotherm of SC800 at higher pressures than those tested. This crossing is observed for CO_2 adsorption, at pressures around 300 kPa.

The lines in Fig. 3 represent the fitting of the virial equation (eqn (1) in the ESI†). Henry's constant (K) quantifies the initial slope of the isotherms and is directly connected with the affinity of the surface for the gas molecules. Thus, the results for K presented in Table 3 quantify the affinity of the materials for CH_4 and CO_2, which were already commented above. In the case of CH_4, the values follow the order SC800 > SC700P > SH800 and for CO_2, the order is SC700P > SC800 > SH800, with K_2CO_3-activated carbons always showing higher affinity for both gases

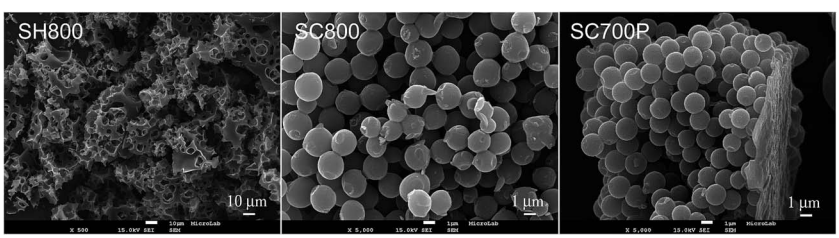

Fig. 2 SEM images of the activated carbon samples.

Table 2 Tap and packing densities of the activated carbons. Calculated methane and carbon dioxide uptake at 1000 kPa and 25 °C (volume of methane or carbon dioxide adsorbed per volume of sample considering the packing density: V/V)

Sample	Tap density (g cm^{-3})	Packing density (g cm^{-3})	CH_4 uptake (V/V)	CO_2 uptake (V/V)
SH800	0.07	0.36	40	99
SC800	0.34	0.79	90	164
SC700P	0.42	0.92	65	108

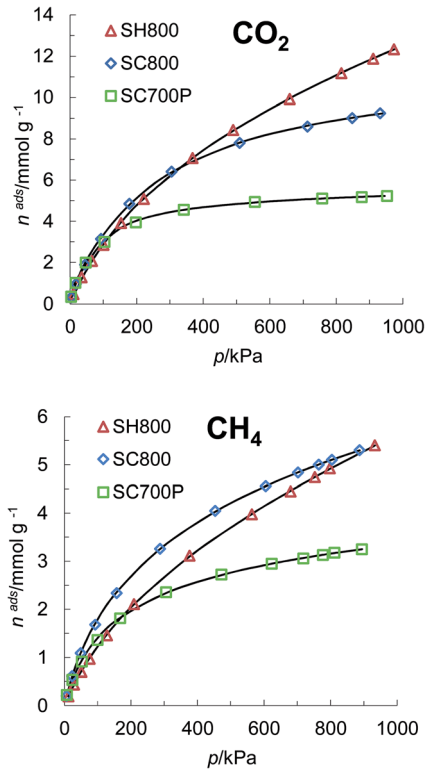

Fig. 3 Carbon dioxide and methane adsorption isotherms at 25 °C on the activated carbons. The lines represent the fitting of the virial equation.

than KOH-activated carbons. The K values obtained for CH_4 (Table 3) are above the average value reported by Matranga *et al.*[35] for a large set of experimental data (1.2×10^{-2} mol kg^{-1} kPa) and above that from simulation data (0.7×10^{-2} mol kg^{-1} kPa), indicating that all obtained samples have a considerable number of active adsorption sites that favor CH_4 adsorption.

Considering the pore network characteristics (Fig. 1 and Table 1), it seems that the sample with the narrower pores (SC700P) is more effective for CO_2 adsorption at low pressures (highest K value for CO_2, Table 3), while the sample with intermediate micropores (SC800) is more effective for CH_4 adsorption at low pressures (highest K value for CH_4, Table 3). In fact, the much high value of K found for the adsorption of CO_2 on SC700P indicates that materials with narrow distributions around 0.5 nm are important for the initial high uptake of this gas. The SC800 case, with the highest value of K for CH_4 adsorption, indicates that materials with pore distributions around 0.6–0.9 nm are more suitable for adsorption of CH_4. Considering the critical molecular size of CO_2 and CH_4, 0.34 nm and 0.38 nm, respectively, one can speculate that in this type of carbon material CO_2 is more prone to absorb in the pores in a single layer fashion, while CH_4 is more prone to adsorb in a double layer fashion.

It has been shown that pores below about 0.7 nm are the ones involved in CH_4 adsorption in activated carbons.[11] However, simulation of CH_4 adsorption on an ideal porous graphite revealed that a pore size of around 0.8 nm is more effective to achieve the highest density of CH_4 adsorbed,[35] giving a theoretical adsorbed amount around 7 mmol g^{-1} at 1000 kPa. Our best result at 1000 kPa (5.5 mmol g^{-1}) is lower than this maximum theoretical value at this pressure and also lower than the value reported for anthracite derived activated carbons optimized for CH_4 storage (7 mmol g^{-1}),[12] although it is significantly higher than the previously reported values for several types of activated carbons (2.5–4.5 mmol g^{-1}).[35] Nevertheless, when a carbon density similar to that found on activated carbons (lower than graphite) is used in the simulation of CH_4 adsorption, the values obtained for adsorbed amounts are about 12% lower[36] and closer to that measured in our best result for sample SC800.

It should be noted that the agreement between the best theoretical pore size (0.8 nm) and the experimental results shown here for CH_4 adsorption also indicates that the method chosen[34] to obtain the micropore size distributions gives meaningful data. Previous attempts using the Dubinin–Stoeckli method to calculate micropore size distributions did not give this agreement,[12] probably due to the predefined Gaussian distribution underlying the Dubinin–Stoeckli method, which is not assumed in the method followed in this work.[34]

Table 3 Virial coefficients and Henry constants for the adsorption of methane and carbon dioxide on the activated carbons[a]

Gas	Sample	K (mol kg^{-1} kPa^{-1})	C_1 (kg mol^{-1})	C_2 (kg mol^{-1})^2	C_3 (kg mol^{-1})^3
CH_4	SH800	1.67×10^{-2}	0.272	−0.014	—
	SC800	3.13×10^{-2}	0.313	—	—
	SC700P	2.61×10^{-2}	0.315	0.090	—
CO_2	SH800	3.98×10^{-2}	0.117	−0.002	—
	SC800	7.85×10^{-2}	0.380	−0.050	0.004
	SC700P	28.3×10^{-2}	1.961	−0.637	0.078

[a] Obtained by the nonlinear least-squares fit of eqn (1) of ESI to the adsorption data.

Selectivity for CO_2–CH_4 mixtures and CH_4 storage

Selectivity and phase diagrams of the separation of CO_2–CH_4 mixtures were estimated from the virial equations, using a method based on Ideal Adsorbed Solution Theory (IAST) detailed elsewhere[9,10] and are briefly summarized in the ESI.† For the SC800 and SH800 samples, the selectivity of the separation is similar in all pressure ranges (Fig. 4). The carbon SC700P presents an initial selectivity close to 7 and then decreases to 4, increasing again with rising pressure to about 6, at 1000 kPa. It is important to emphasize that, although SC700P presents modest adsorbed amounts compared to the other samples (Fig. 3), the selectivity of the separation on this sample is significantly better. In fact, this carbon presents a selectivity that is above the value of 3 that is considered as a reference for industrial feasibility,[37] while the other samples only reach close to this value at the highest pressure tested. The difference among samples is further illustrated in Fig. 5 where it can be seen that SC700P presents an improved performance over the other samples. For example, considering the separation of a gas mixture with 0.5 molar composition (y_{CH_4}), typical for bio and landfill gases, the composition in the adsorbed phase (x_{CH_4}) is 0.15 on SC700P and about 0.25 on SH800 and SC800, at 500 kPa and 25 °C. This means that the adsorbed phase on SC700P is richer in CO_2 (0.85) than that on SH800 and SC800 (0.75). Clearly, the narrow pore size distribution of the SC700P sample is responsible for the interesting selectivity for the mixture separation.

For applications, it is often useful to compare the adsorbents regarding their gas storage capacity as the volume of gas retained in the material per volume of storage vessel or separation column. The importance of the density on the evaluation of the volumetric storage capacity of a given material was recently highlighted in the work of Kunowsky *et al.*[38] For this kind of comparison, in our work the packing density has been taken into account to express the adsorbed amounts per volume of the adsorbent material. When the adsorbed amounts are converted to gas volume (Standard Temperature and Pressure – STP), the volume of gas retained in a given adsorbent volume can be calculated on a V/V basis.

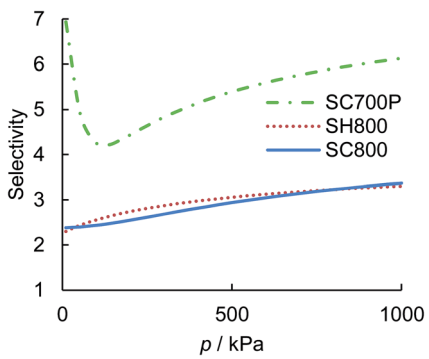

Fig. 4 Average selectivity for the CO_2–CH_4 separation on the activated carbons.

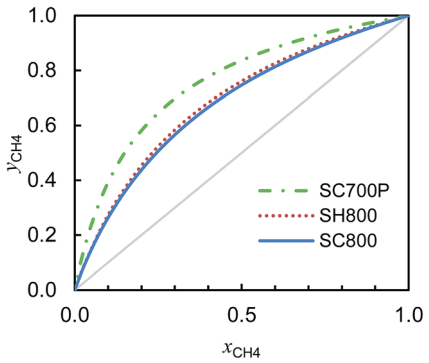

Fig. 5 Isothermal (25 °C), isobaric (500 kPa) *xy* phase diagrams of the CO_2–CH_4 mixtures on the activated carbons. y_{CH_4} is the molar faction of methane in the gas phase; x_{CH_4} is the molar faction of methane in the adsorbed phase.

These results show a very different trend of the isotherms (Fig. 6). Comparing these last ones with the previously presented isotherms where the adsorbed amount is expressed per gram of material (Fig. 3), it can be seen that the KOH-activated sample (SH800) presents a significant decrease in the volume adsorbed (Fig. 6) for both gases, in relation to the K_2CO_3-activated carbons, due to its much lower packing

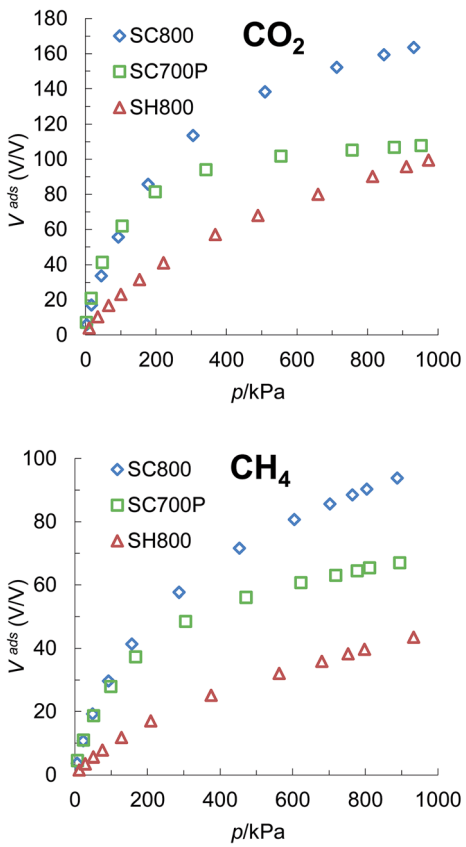

Fig. 6 Carbon dioxide and methane adsorption isotherms at 25 °C on the activated carbons, taking into account the density of the materials and expressing the amounts adsorbed per unit volume of material.

density among the materials (Table 2). So, although presenting the highest adsorbed amounts per gram of sample (Fig. 3), the low packing density of carbon SH800 makes it unsuitable for some applications, where the volume of the adsorbent material is a limiting factor, as is the case of gas storage.

The curves in V/V (Fig. 6) highlight the potentialities of the K_2CO_3-activated samples, as they present significantly higher volumes adsorbed per volume of material than the sample activated with KOH. It is well known that KOH activation tends to give activated carbons with high surface areas and essentially microporous nature. However, in the particular case of sucrose-derived hydrochars, KOH destroys the spherical structure of the hydrochar (Fig. 2) hindering an efficient packing of the particles, thus giving low packing densities. K_2CO_3 appears to be a better activating agent because the spherical structure is maintained and still gives high surface areas (Table 1). The combination of these two features gives K_2CO_3 activated hydrochars an enhanced storage capacity (V/V) when compared to KOH activation reported in this work and in a previously published study.[13] In fact, the best CH_4 storage value obtained in the present work for the SC800 sample (90 (V/V), Table 2) at 1000 kPa is higher than that reported by Falco *et al.*[13] (between 43 and 53 (V/V), both values calculated from reported adsorbed amounts at 1000 kPa and the packing densities) and interestingly similar to those observed on anthracite derived carbons activated with KOH (82 (V/V)),[12] at the same pressure. Comparing the storage capacity (Table 2) and the surface area (Table 1) of the materials, it is evident that the surface area is not the only parameter ruling the CH_4 storage capacity. This is due to the influence of the packing density, already discussed, and also due to the lower density of CH_4 in supermicropores[11] present in the material with the highest surface area (SH800).

Considering the upgrade of natural, landfill or biogas, the activated carbons can be evaluated regarding the composition of the adsorbed phase. For this, the volume of each gas adsorbed (V/V) was estimated as a function of the composition of the gas phase (Fig. 7). Once again, the KOH-activated carbon (SH800) presents lower adsorbed volumes than the K_2CO_3-activated carbons (SC800 and SC700P). More interesting is the performance of the SC700P sample that presents a combination of high CO_2 adsorbed volumes and an adsorbed phase richer in CO_2 in a wide range of gas composition. A detailed comparison of the plots in Fig. 7 shows that the crossing point at which the concentration of CO_2 in the adsorbed phase becomes lower than that of CH_4 is obtained at a higher molar fraction of CH_4 in the gas phase (0.85) for the SC700P sample. This means that, during CO_2–CH_4 separation, this sample will retain more CO_2 than CH_4 in a wider range of feed compositions than the other tested samples. For practical applications, although K_2CO_3-activated carbon SC700P presents lower adsorbed amounts per grams and lower surface area and pore volumes, due to its high density and selectivity it appears as the most promising material for CO_2–CH_4 separation.

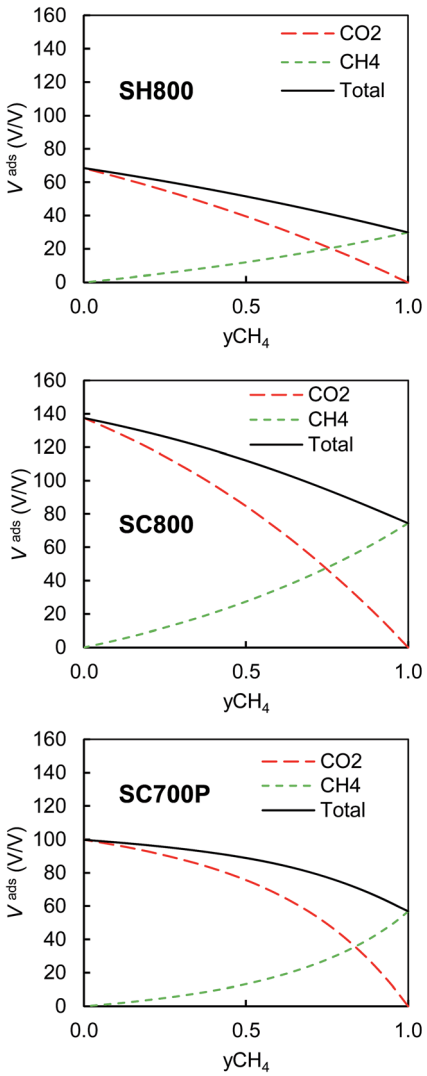

Fig. 7 Adsorbed amounts of the CO_2–CH_4 mixture as a function of the CH_4 molar fraction in the gas phase, at 500 kPa and 25 °C, for the activated carbons.

Conclusions

K_2CO_3 activation of sucrose-derived hydrochars allows the preparation of materials preserving the microspherical morphology, along with high porosity development and specific properties suitable to be used in CO_2–CH_4 separation. Moreover, the spherical morphology leads to high packing densities, a crucial parameter for high gas storage volume (V/V), which is particularly important for CH_4 storage. Conversely, the KOH activated sample (SH800) has lower preparation yield and density that leads to lower storage volumes (V/V) and wider micropores less favourable for CO_2–CH_4 separation.

Furthermore, the micropore size distributions assessed from CO_2 adsorption data without imposing a Gaussian distribution reveal that the sample presenting the best CH_4 adsorption capacity (SC800) is also the one for which the maximum is centered in the predicted pore width for enhanced CH_4 storage (0.8 nm). Considering the micropore size distribution, it seems

that the microspherical activated carbon (SC700P) with a narrow pore distribution centered at 0.5–0.6 nm is more suitable for application in the CO_2–CH_4 separation.

Besides the applications herein described, the properties of K_2CO_3-activated hydrochar samples allow envisaging their use in other processes. These carbons combine the spherical morphology with very narrow micropore size distributions, so they can present molecular sieves properties. On the other hand, their acidic surface chemistry opens new possibilities for their use in other adsorption processes or for the synthesis of functional carbon-based materials.

Acknowledgements

The authors thank Fundação para a Ciência e Tecnologia, Portugal, for financial support through projects PEst-OE/QUI/UI0612/2013 (CQB) and Pest-C/EQB/LA0006/2011 (REQUIMTE) and Operation NORTE-07-0124-FEDER-000067 – NANOCHEMISTRY. ASM thanks FCT for the Post-doc grant SFRH/BPD/86693/2012. MLP thanks FEDER, QREN, COMPETE, and FCT for financial support to CICECO project FCOMP-01-0124-FEDER-037271 (PEst-C/CTM/LA0011/2013) and Investigador FCT contract IF/00993/2012/CP0172/CT0013.

References

1 J. Bekkering, A. A. Broekhuis and W. J. T. van Gernert, *Bioresour. Technol.*, 2010, **101**, 450–456.
2 K. S. Knaebel and H. E. Reinhold, *Adsorption*, 2003, **9**, 87–94.
3 S. Matar and L. F. Hatch, *Chemistry of Petrochemical Processes*, Gulf Publishing Company, Houston, 2000.
4 P. Weiland, *Appl. Microbiol. Biotechnol.*, 2010, **85**, 849–860.
5 Commission Directive 2001/27/EC of 10 April 2001.
6 W. T. Tsai, *Renewable Sustainable Energy Rev.*, 2007, **11**, 331–344.
7 W. Qin, F. N. Egolfopoulos and T. T. Tsotsis, *Chem. Eng. J.*, 2001, **82**, 157–172.
8 V. K. Saini, M. Pinto and J. Pires, *Green Chem.*, 2011, **13**, 1251–1259.
9 J. Pires, V. K. Saini and M. L. Pinto, *Environ. Sci. Technol.*, 2008, **42**, 8727–8732.
10 M. L. Pinto, J. Pires and J. Rocha, *J. Phys. Chem. C*, 2008, **112**, 14394–14402.
11 J. Alcañiz-Monge, D. Lozano-Castelló, D. Cazorla-Amorós and A. Linares-Solano, *Microporous Mesoporous Mater.*, 2009, **124**, 110–116.
12 D. Lozano-Castelló, D. Cazorla-Amorós, A. Linares-Solano and D. F. Quinn, *Carbon*, 2002, **40**, 989–1002.
13 C. Falco, J. P. Marco-Lozar, D. Salinas-Torres, E. Morallón, D. Cazorla-Amorós, M. M. Titirici and D. Lozano-Castelló, *Carbon*, 2013, **62**, 346–355.
14 M. Sevilla and A. B. Fuertes, *Energy Environ. Sci.*, 2011, **4**, 1765–1771.
15 M. Jorda-Beneyto, D. Lozano-Castello, F. Suarez-Garcia, D. Cazorla-Amorós and A. Linares-Solano, *Microporous Mesoporous Mater.*, 2008, **112**, 235–242.
16 M. Galhetas, A. S. Mestre, M. L. Pinto, I. Gulyurtlu, H. Lopes and A. P. Carvalho, *Chem. Eng. J.*, 2014, **240**, 344–351.
17 A. S. Mestre, A. S. Bexiga, M. Proença, M. Andrade, M. L. Pinto, I. Matos, I. M. Fonseca and A. P. Carvalho, *Bioresour. Technol.*, 2011, **102**, 8253–8260.
18 I. Cabrita, B. Ruiz, A. S. Mestre, I. M. Fonseca, A. P. Carvalho and C. O. Ania, *Chem. Eng. J.*, 2010, **163**, 249–255.
19 A. S. Mestre, J. Pires, J. M. F. Nogueira and A. P. Carvalho, *Carbon*, 2007, **45**, 1979–1988.
20 A. P. Carvalho, M. Gomes, A. S. Mestre, J. Pires and M. Brotas de Carvalho, *Carbon*, 2004, **42**, 672–674.
21 A. S. Mestre, R. A. Pires, I. Aroso, E. M. Fernandes, M. L. Pinto, R. L. Reis, M. A. Andrade, J. Pires, S. P. Silva and A. P. Carvalho, *Chem. Eng. J.*, 2014, **253**, 408–417.
22 M. A. Andrade, R. J. Carmona, A. S. Mestre, J. Matos, A. P. Carvalho and C. O. Ania, *Carbon*, 2014, **76**, 183–192.
23 M. Galhetas, A. S. Mestre, M. L. Pinto, I. Gulyurtlu, H. Lopes and A. P. Carvalho, *J. Colloid Interface Sci.*, 2014, DOI: 10.1016/j.jcis.2014.06.043.
24 A. S. Mestre, C. Freire and A. P. Carvalho, *EcoCarbons: Hydrothermal carbonization of carbohydrates, Abstracts of the XXXIV Reunión Bienal Real Sociedad Española de Química (Oral presentation)*, Santander (Spain), 2013.
25 D. Adinata, W. M. A. W. Daud and M. K. Aroua, *Bioresour. Technol.*, 2007, **98**, 145–149.
26 H. Marsh and F. Rodríguez-Reinoso, *Activated Carbon*, Elsevier, Oxford, 2006.
27 S. J. Gregg and K. S. W. Sing, *Adsorption, Surface Area and Porosity*, Academic Press Inc., London, 1982.
28 L. Gurvich, *J. Russ. Phys.–Chem. Soc.*, 1915, **47**, 805–827.
29 F. Rodríguez-Reinoso, J. M. Martin-Martinez, C. Prado-Burguete and B. McEnaney, *J. Phys. Chem.*, 1987, **91**, 515–516.
30 J. Wang and S. Kaskel, *J. Mater. Chem.*, 2012, **22**, 23710–23725.
31 D. Lozano-Castello, J. M. Calo, D. Cazorla-Amorós and A. Linares-Solano, *Carbon*, 2007, **45**, 2529–2536.
32 E. Raymundo-Pinero, P. Azais, T. Cacciaguerra, D. Cazorla-Amorós, A. Linares-Solano and F. Béguin, *Carbon*, 2005, **43**, 786–795.
33 F. Rodríguez-Reinoso, in *Carbon and Coal Gasification: Science and Technology*, ed. J. L. Figueiredo and J. A. Moulijn, Martinus Nijhoff, Drodrecht, 1986.
34 M. L. Pinto, A. S. Mestre, A. P. Carvalho and J. Pires, *Ind. Eng. Chem. Res.*, 2010, **49**, 4726–4730.
35 K. R. Matranga, A. L. Myers and E. D. Glandt, *Chem. Eng. Sci.*, 1992, **47**, 1569–1579.
36 X. S. Chen, B. McEnaney, T. J. Mays, J. Alcaniz-Monge, D. Cazorla-Amorós and A. Linares-Solano, *Carbon*, 1997, **35**, 1251–1258.
37 R. T. Yang, *Gas Separation by Adsorption Processes*, Butterworths Publishers, Boston, 1987.
38 M. Kunowsky, F. Suarez-Garcia and A. Linares-Solano, *Microporous Mesoporous Mater.*, 2013, **173**, 47–52.

